

Temporal and spatial evolution of C₂ in laser induced plasma from graphite target

S. S. Harilal, Riju C. Issac, C. V. Bindhu, V. P. N. Nampoori, and C. P. G. Vallabhan^{a)}
*Laser Division, International School of Photonics, Cochin University of Science & Technology,
Cochin 682 022, India*

(Received 26 February 1996; accepted for publication 10 June 1996)

Laser ablation of graphite has been carried out using 1.06 μm radiation from a *Q*-switched Nd:YAG laser and the time of flight distribution of molecular C₂ present in the resultant plasma is investigated in terms of distance from the target as well as laser fluences employing time resolved spectroscopic technique. At low laser fluences the intensities of the emission lines from C₂ exhibit only single peak structure while beyond a threshold laser fluence, emission from C₂ shows a twin peak distribution in time. The occurrence of the faster velocity component at higher laser fluences is explained as due to species generated from recombination processes while the delayed peak is attributed to dissociation of higher carbon clusters resulting in the generation of C₂ molecule. Analysis of measured data provides a fairly complete picture of the evolution and dynamics of C₂ species in the laser induced plasma from graphite. © 1996 American Institute of Physics. [S0021-8979(96)02218-9]

I. INTRODUCTION

The interaction of high power laser beams with a graphite target has become a subject of great interest since the first report on the existence of stable carbon clusters called fullerenes in laser ablated plasma from graphite.¹⁻⁵ It has been found that when a graphite surface is vaporized by intense laser pulses in a helium atmosphere of moderate pressure remarkably stable carbon clusters are produced.^{6,7} Many experimental⁸⁻¹¹ and theoretical studies¹²⁻¹⁴ on the structure and stability of these species have been made recently. Depending upon the time of observation, position of the sampled volume within the plasma, and fluence of irradiation the relative abundance of the different types of carbon clusters has been found to change. The plasma temperature and the number densities of different species in laser produced plasmas from graphite targets have already been reported^{15,16}. Pulsed laser ablation of high purity graphite is also found to be one of the effective methods for the preparation of diamond-like carbon (DLC) thin films.¹⁷⁻²² An improved knowledge of the dynamics of laser interaction with materials is important for the purpose of optimizing the conditions for depositing high quality DLC films. Nevertheless, the studies on laser produced carbon plasma have not yet yielded a clear picture of the dynamics of cluster formation and such a situation is evidently due to the complexity of the phenomena involved^{16,23,24}. In order to understand the processes leading to cluster formation, which may directly influence laser deposition, the mechanism of plasma plume generation from the target material under laser irradiation and the interaction of the resulting plume with the ambient atmosphere in the plasma chamber should be studied in detail. There are several techniques for characterizing laser induced plasma and these include optical emission spectroscopy,²⁵⁻²⁷ optical absorption spectroscopy,^{28,29} laser induced fluorescence,^{30,31} time resolved spectroscopy,³² mass

spectroscopy³ etc. Among these, time resolved spectroscopy is the most suitable method to study the dynamics of laser produced plasma. In this paper we report some interesting results obtained from the time and space resolved spectroscopic analysis of C₂ species in the laser induced plasma produced from a high purity graphite target using 1.06 μm radiation from a pulsed Nd:YAG laser. We highlight here especially the occurrence of multiple peak structure in the temporal profile of C₂ emission.

II. EXPERIMENTAL SETUP

The details of the experimental setup have been described elsewhere.^{32,33} The graphite target having a diameter of 15 mm and thickness 3 mm is mounted inside a stainless steel vacuum chamber equipped with quartz windows in such a way that the target surface could be irradiated at normal incidence using a 1.06 μm laser beam from a *Q*-switched Nd:YAG laser having pulse width 9 ns and pulse repetition frequency 10 Hz. The sample is rotated about an axis parallel to the laser beam to avoid local heating and pitting. The pressure inside the plasma chamber is kept at 100 mTorr of helium during the entire series of observations. The emission spectrum from graphite plasma is viewed normal to its expansion direction and imaged using appropriate focusing lenses and apertures onto the slit of a 1 meter monochromator (Spex, Model 1702) which is coupled to a thermoelectrically cooled photomultiplier tube (PMT, Thorn EMI model KQB 9863, rise time 2 ns). For spatially resolved studies, different regions of the plasma plume are focused onto the monochromator slit. In our studies the accuracy in spatial position is better than 0.2 mm. The characteristic lines of the species are selected by the monochromator and the PMT output is fed to a 200 MHz digital storage oscilloscope (Iwatsu model DS 8621) provided with a 50 ohm termination to record the emission pulse shapes. This setup essentially provides delay as well as decay times for the emission from

^{a)}Electronic mail: root@cochin.ernet.in

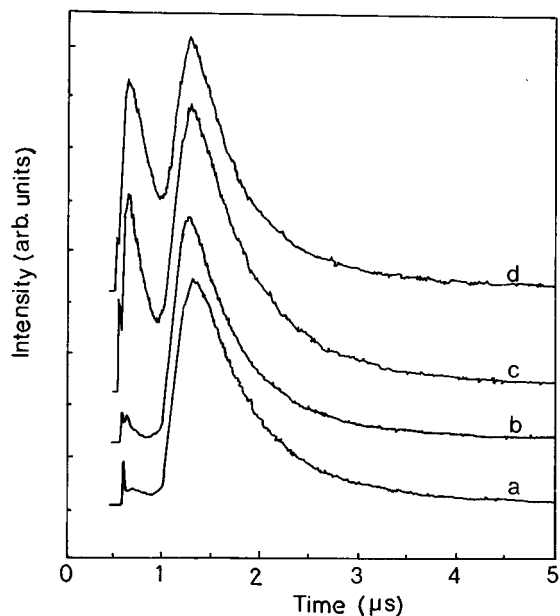


FIG. 1. Intensity variation with time for 516.5 nm spectral emission from C_2 observed at 5 mm away from the target for laser fluences (a) 12.7 $J cm^{-2}$, (b) 26.7 $J cm^{-2}$, (c) 28 $J cm^{-2}$, and (d) 29.3 $J cm^{-2}$.

constituent species at a specific point within the plasma. These are extremely important parameters related to the evolution of laser ablated materials.

III. RESULTS AND DISCUSSION

The time resolved studies of emission lines from various species are carried out from the oscilloscope traces which show definite time delays for emission with respect to the incidence of the laser pulse. Our observations show that the emission lines from different emitting species within the plasma possess distinctly different temporal profiles. Each temporal profile represents a complex convolution of different factors that govern the temporal history of the emitting species viz. its production mechanism and rate, its flight past the viewing region and its radiative and collisional decay rates. Typical time of flight (TOF) distributions of C_2 species obtained by monitoring the spectral emission from C_2 in electronic excited state ($d^3\Pi_g$) [at $\lambda = 516.5$ nm corresponding to the (0, 0) transition $d^3\Pi_g \rightarrow a^3\Pi_u$ of the C_2 Swan system] at a distance of 5 mm from the target for different laser fluences are given in Fig. 1. The initial spike in the figure is due to scattering and can be used as a time marker. The interesting feature in TOF pattern of C_2 species is its double peak structure which becomes prominent beyond a threshold laser fluence. In what follows first peak is designated as P1 and delayed peak P2. Such double peak structure has already been reported by some of the earlier workers.³⁴⁻³⁶ However, our observations bring out certain novel features which are described below.

(1) The time delay for P1 with respect to the separation between the point of observation and the target surface varies in a nonlinear manner; the nonlinearity being more pronounced at lower laser fluences. As is evident from Fig. 2,

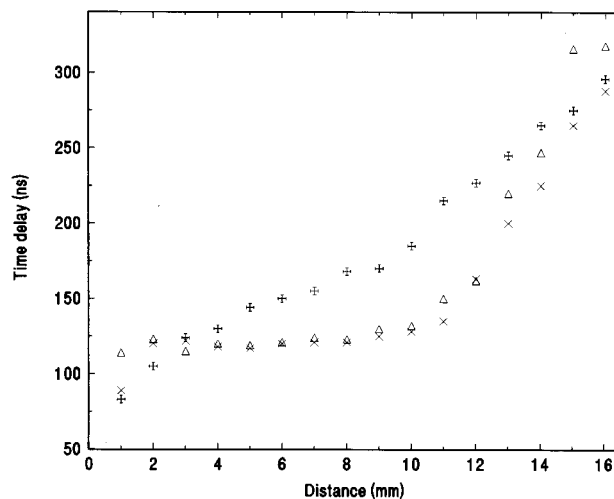


FIG. 2. Variation of time delays with distance of P1 for different laser fluences (\times) 29.3 $J cm^{-2}$, (Δ) 31.6 $J cm^{-2}$ and ($+$) 34.4 $J cm^{-2}$.

the delay of P1 almost constant up to 10 mm separation which is paradoxical while the delay of P2 varies almost linearly (Fig. 3) with such separation.

(2) The delay of P1 increases with laser fluence (Fig. 4) while that of P2 (Fig. 5), decreases sharply after being constant up to a certain value of laser fluence.

(3) Appearance of P1 occurs only beyond a threshold fluence of about 26.7 $J cm^{-2}$ at 5 mm away from the target ($z = 5$ mm) and this threshold value increases with increasing distance from the target.

(4) The intensity for P1 is maximum at a point around $z = 12$ mm (Fig. 6) for all values of laser fluences while that of P2 attains maximum around $z = 5$ mm (Fig. 7).

(5) The intensity of P1 increases from zero (at fluence about 26.7 $J cm^{-2}$) and saturates at higher fluences (>30.55 $J cm^{-2}$) (Fig. 8) while that of P2 increases up to an optimum laser fluence and begins to decrease thereafter

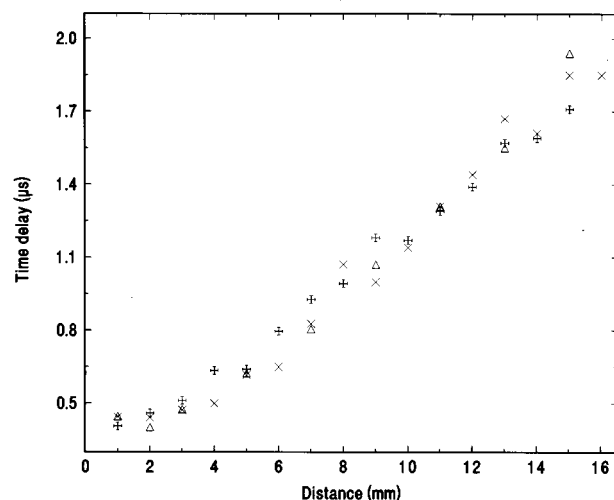


FIG. 3. Variation of time delays with distance of P2 for different laser fluences (\times) 29.3 $J cm^{-2}$, (Δ) 31.8 $J cm^{-2}$ and ($+$) 34.4 $J cm^{-2}$.

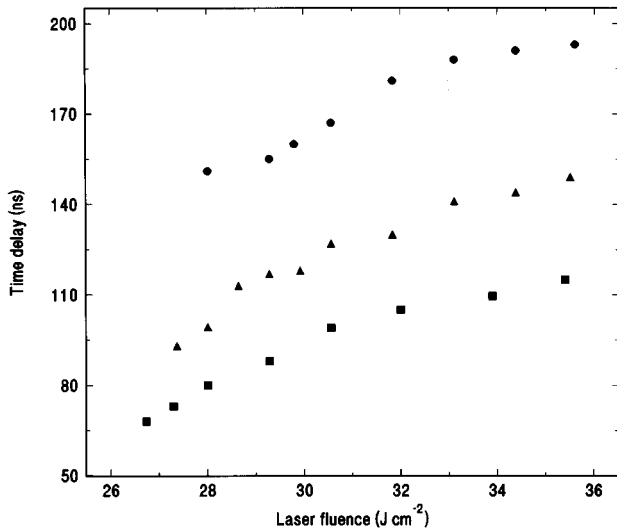


FIG. 4. Plot of time delays on laser fluence of P1 for different distances (■) 5 mm, (▲) 10 mm and (●) 15 mm.

(Fig. 9). This behavior is predominant at points having smaller separation from the target.

The above observations indicate that the plasma apparently develops a fast and slow component above a threshold laser fluence. In fact the existence of a twin peak structure for the C_2 species from the laser induced plasma observed previously has been explained as due to emission from the “shell” (fast) and the “core” (slow) components.³⁴ Attributing peaks P1 and P2 solely to fast and slow components will not explain the unusual spatial dependence of time delays as depicted in Figs. 2 and 3, respectively.

At low laser fluences, clusters of carbon atoms (C_n) along with electrons are ejected from the graphite and C_2 could be formed by the dissociation of $C_n (n > 2)$ due to collisions with energetic electrons.³⁷ The larger masses of C_n will result in longer delays which are observed in the C_2

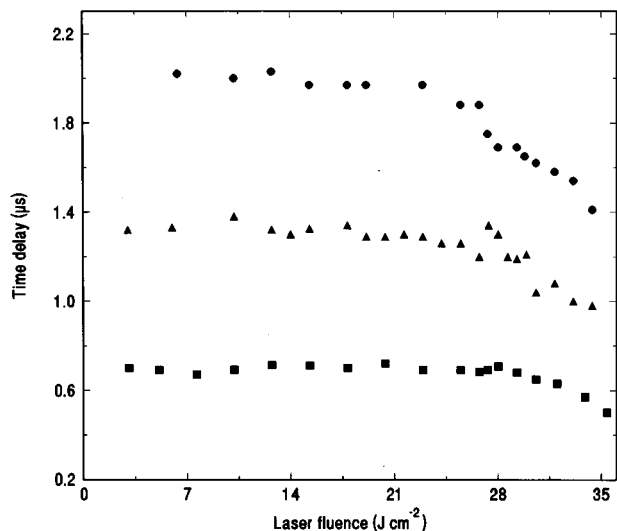


FIG. 5. Plot of time delays on laser fluence of P2 for different distances (■) 5 mm, (▲) 10 mm and (●) 15 mm.

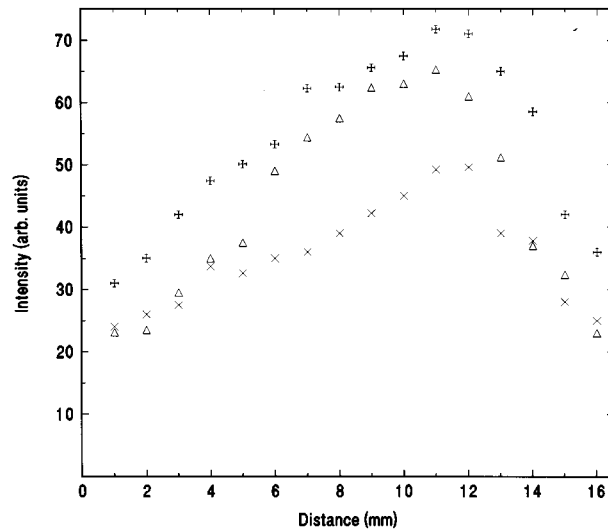


FIG. 6. Change in intensity with distance for different laser fluences for the peak P1 (×) 29.3 J cm^{-2} , (Δ) 31.8 J cm^{-2} and (+) 34.4 J cm^{-2} .

emission (peak P2) occurring at the lower laser fluences. Above a distance ≈ 6 mm from the target, the plasma is colder compared with the same in core region and collisional effects become insufficient to cause dissociation of C_n . As the laser fluence is increased, clusters with lower values of n will be ejected directly from the target. Above a threshold laser fluence, temperature of the plasma becomes so large so as to dissociate C_n to neutral and ionized carbon atoms just outside the target. It is in fact observed that the emission intensity of the ionized species does increase drastically above this threshold laser fluence. Once ions and electrons are produced, one can have neutral carbon atoms by three body collision processes like



Collisional ionization is also possible through processes like

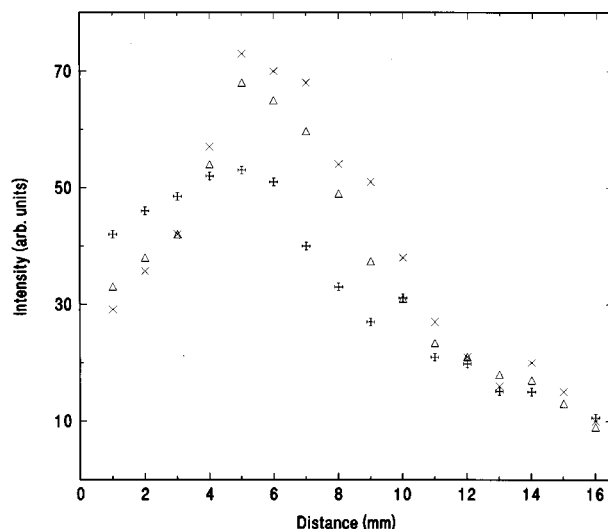


FIG. 7. Change in intensity with distance for different laser fluences for the peak P2 (×) 29.3 J cm^{-2} , (Δ) 31.8 J cm^{-2} and (+) 34.4 J cm^{-2} .

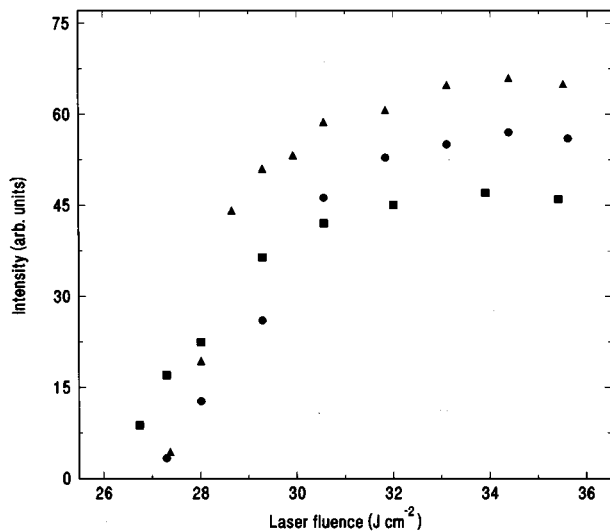


FIG. 8. Variation of intensity of P1 with laser fluence for (■) 5mm, (▲) 10 mm and (●) 15 mm.



In the vicinity of the target, Eq. (2) may be predominant over Eq. (1) so that we get excited state C_2 formation slightly away from the target, giving emission peak P1. The threshold like phenomenon in the case of P1 also shows the initiation of production of ionized species so as to open the channels (1) and (2) at higher laser fluences. As the laser fluence is increased beyond 26.7 J cm^{-2} , the probability of cluster formation of the type $C_n (n > 2)$ in the plasma diminishes, thereby causing a drastic decrease in the intensity of P2. Moreover, as the laser fluence is increased, the trailing edge of the laser pulse will enhance the dissociation of C_n by multiphoton absorption through laser plasma interaction. This could cause the formation of C_2 nearer the target surface. Koren and Yeh³⁴ also have observed such double peaks in the case of C_2 from polyimide target and their interpreta-

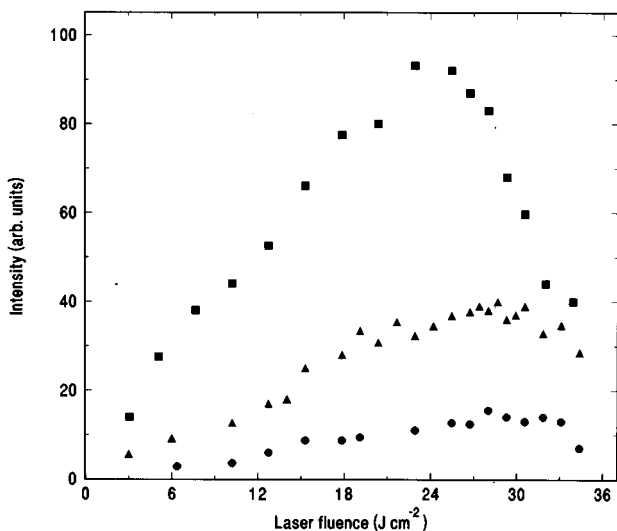


FIG. 9. Variation of intensity of P2 with laser fluence for (■) 5mm, (▲) 10 mm and (●) 15 mm.

tion in terms of the fast and slow components does not completely explain our observations. We are therefore compelled to attribute the double peak formation due to the delays inherent in the distinctly different formation mechanisms of C_2 in the plasma.

Figs. 4 and 5 give respectively the variation in time delay for P1 and P2 with laser fluence for different distances from the target. From Fig. 4, we see that the time delay for P1 increases with respect to increase in laser fluence which is against the normal observation where velocity usually increases with the fluence of the incident laser pulse. By considering the velocity distribution, this anomaly can be explained only if one can have some type of a “negative diffusion” or anomalous diffusion of C_2 towards the target. Similar observations by one of the previous workers have been explained as due to selective depletion of high velocity C_2 species.³⁸ However, one can have a slightly different scenario as explained below. As the laser fluence increases, the electron, atom and ion number densities of the plasma and plasma temperature are also increased. This may cause larger probability for events (1) and (2) indicated in the previous paragraph. It is also believed that ions are accelerated by Coulomb fields generated by fast moving electrons escaping from the plume. One should also consider the multiphoton dissociation of C_n by the trailing edge of the laser pulse so as to produce C_2 nearer to the target surface. Due to these processes C_2 may thus be formed at points nearer to the target surface by recombination process, but with more than usual delay in the appearance of P1. In other words, decrease in delay with laser fluence competes with the increase in delay due to shift of “formation site” of C_2 nearer to the target surface. Therefore, as far as P1 is concerned, delay due to the location of formation site is more predominant in the range of laser fluences considered here, thereby causing the observed enhancement in the delay on increasing the laser fluence. This is further born out by the fact that there is a perceptible increase in the half width of peak P1 as the fluence of the laser pulse is increased.

Similar arguments can be made in the case of the measured time delays corresponding to P2. Contrary to the case of P1, delay of P2 remains almost constant up to a threshold laser fluence and thereafter it decreases. As noted earlier P2 is found to be formed due to dissociation of carbon clusters $C_n (n > 2)$. As the laser fluence is increased the formation of C_2 through dissociation of C_n will occur nearer to the target surface, thereby causing an increase in the delay as opposed to its decrease due to enhancement of kinetic energy of the species with laser fluence. Up to a threshold laser fluence, these two time delays are more or less balanced to give an effectively constant time delay as observed in Fig. 5. Above this fluence threshold, enhancement in kinetic energy becomes so large that there will be a notable decrease in time delay for P2.

The nature of variation of delay with distance also exhibits evidently certain peculiarities in terms of the behavior of peaks P1 and P2 (Figs. 2 and 3). Beyond a distance of 8 mm there is a sudden enhancement in delay for P1 especially at comparatively lower fluences but well above the threshold. The unusual spatial dependence of time delay is observed

only for P1 and the variation differs widely as the laser fluence is changed. However for P2 the nearly linear spatial dependence of the delay is observed. The plots of delay time as a function of position show that the velocities of the species producing P1 and P2 increase with spatial separation from the target until it reaches distances 11 mm and 6 mm respectively and then the expansion velocity is found to be almost constant ($V_{P1} = 6.5 \times 10^4$ m/s, $V_{P2} = 8 \times 10^3$ m/s). The intensity variation for the peaks P1 and P2 with respect to distance is shown in Figures 6 and 7. The spatial maximum (the distance at which the intensity of the peak is maximum) of P1 is at about 12 mm while that for P2 is at 6 mm. It is also clear from Fig. 9 that the intensity of P2 decreases after the threshold laser fluence where as intensity of P1 increases from zero (at 26.7 J cm^{-2} for $z = 5$ mm) and saturates at higher laser fluences (Fig. 8). It indicates a decrease in the population of $C_n (n > 2)$ when laser fluence is increased (Fig. 9). The saturation effect of plasma emission can be explained as due to the absorption of the trailing part of the laser radiation by the plasma. This absorption will be more pronounced at higher plasma densities so that effective laser power reaching the target will be reduced. Such ‘shielding effect’ of target from the laser radiation will result in the observed saturation effect.

IV. CONCLUSIONS

We have observed double peak structure in the temporal history of emission from electronically excited C_2 molecules in laser induced plasma produced from a graphite target. The present work clearly points to the existence of the various mechanisms of the formation of C_2 species in the plasma. At low incident laser fluences C_2 formation is mainly due to dissociation of higher carbon clusters while at higher laser fluences the C_2 formation is due to many body recombination. Formation of C_2 due to the dissociation of higher clusters leads to the presence of the delayed component which occur at all laser fluences. Those created by recombination processes apparently give rise to a faster components with a corresponding emission peak which appears only at higher fluences. We have also observed the effect of helium in the plasma dynamics. Collision between helium atoms and other species in the plasma does influence the spatial and temporal features of emission from C_2 . The details of this aspect will be dealt with separately in later communication.

ACKNOWLEDGMENTS

The present work is supported by the Department of Science and Technology, Government of India. One of the authors (SSH) is grateful to Council of Scientific and Industrial Research, New Delhi for a senior research fellowship. RCI and CVB are thankful to University Grant Commission, New Delhi for their research fellowships.

- ¹H. W. Kroto, R. J. Heath, S. C. O'Brien, R. F. Curl, and R. E. Smalley, *Nature* **318**, 165 (1985).
- ²G. Meier and D. S. Betune, *J. Chem. Phys.* **93**, 7851 (1990).
- ³E. A. Rohlfing, *J. Chem. Phys.* **93**, 7851 (1990).
- ⁴H. W. Kroto and K. G. Mikay, *Nature* **331**, 328 (1988).
- ⁵W. Kratschmer, L. D. Lamb, K. Fostiropoulos, and D. R. Huffman, *Nature* **347**, 354 (1990).
- ⁶W. Weltner, Jr. and R. J. Van Zee, *Chem. Rev.* **89**, 1713 (1989).
- ⁷H. W. Kroto, A. N. Allat, and S. P. Balm, *Chem. Rev.* **91**, 1213 (1991).
- ⁸S. C. O'Brien, J. R. Heath, R. F. Curl, and R. E. Smalley, *J. Chem. Phys.* **88**, 220 (1988).
- ⁹Q. L. Zhang, S. C. O'Brien, J. R. Heath, Y. Liu, R. F. Curl, H. W. Kroto, and R. E. Smalley, *J. Chem. Phys.* **90**, 525 (1986).
- ¹⁰D. M. Cox, K. C. Reichmann, and A. Kaldor, *J. Chem. Phys.* **88**, 1588 (1988).
- ¹¹E. A. Rohlfing, D. M. Cox, and A. Kaldor, *J. Chem. Phys.* **81**, 3322 (1984).
- ¹²F. Negri, G. Orlandi, and F. Zerbetto, *Chem. Phys. Lett.* **144**, 31 (1988).
- ¹³D. E. Weeks and W. G. Hartner, *Chem. Phys. Lett.* **144**, 366 (1988).
- ¹⁴T. G. Schmalz, N. A. Seitz, D. J. Klein, and G. E. Hite, *J. Am. Chem. Soc.* **110**, 113 (1988).
- ¹⁵E. A. Rohlfing, *J. Chem. Phys.* **89**, 6103 (1988).
- ¹⁶M. Anselment, R. S. Smith, E. Daykin, and L. F. Dimamo, *Chem. Phys. Lett.* **134**, 444 (1983).
- ¹⁷W. A. Creasy and J. T. Brenna, *J. Chem. Phys.* **92**, 2269 (1990).
- ¹⁸G. Dollinger and P. Maier-Komor, *Nucl. Instrum. Methods Phys. Res. A* **303**, 50 (1991).
- ¹⁹G. Dollinger, C. M. Frey, and P. Maier-Komor, *Nucl. Instrum. Methods Phys. Res. A* **334**, 167 (1993).
- ²⁰T. Sato, S. Furuno, S. Iguchi, and M. Hanabusa, *Jpn. J. Appl. Phys.* **26**, L1487 (1987).
- ²¹D. L. Pappas, K. L. Saenger, J. Bruley, W. Krakow, and J. J. Cuomo, *J. Appl. Phys.* **71**, 5675 (1992).
- ²²F. Daranloo, E. M. Juengerman, D. R. Jander, T. J. Lee, and C. B. Collins, *J. Appl. Phys.* **67**, 2081 (1990).
- ²³R. Teghil, A. Giardini-Guidoni, S. Piccirillo, A. Mele, and F. Polla-Mattiot, *Appl. Surf. Sci.* **46**, 220 (1990).
- ²⁴P. S. R. Prasad, Abhilasha, and R. K. Thareja, *Phys. Status Solidi A* **139**, K1 (1993).
- ²⁵Y. Tasaka, M. Tahako, and S. Usami, *Jpn. J. Appl. Phys.* **34**, 1673 (1995).
- ²⁶V. N. Anisimov, V. Y. Baranov, V. G. Grishina, O. N. Delkash, A. Y. Serbrant, and M. A. Stepanova, *Appl. Phys. Lett.* **67**, 2923 (1995).
- ²⁷S. S. Harilal, R. C. Isaac, C. V. Bindhu, V. P. N. Nampoori, and C. P. G. Vallabhan, *Pramana, J. Phys.* **46**, 145 (1996).
- ²⁸T. Morrow, H. F. Sakeek, A. El Astal, W. G. Graham, and D. G. Walmsley, *J. Supercond.* **7**, 238 (1994).
- ²⁹D. B. Geohegan, *Laser Ablation: Mechanisms and Applications* (Springer, Heidelberg, 1991), p. 28.
- ³⁰J. E. H. Goldsmith and D. T. B. Kearsley, *Appl. Phys. B* **50**, 371 (1990).
- ³¹Y. Nakata, W. K. A. Kumuduni, T. Okada, and M. Meada, *Appl. Phys. Lett.* **66**, 3206 (1995).
- ³²S. S. Harilal, P. Radhakrishnan, V. P. N. Nampoori, and C. P. G. Vallabhan, *Appl. Phys. Lett.* **64**, 3377 (1994).
- ³³G. Padmaja, A. V. Ravi Kumar, P. Radhakrishnan, V. P. N. Nampoori, and C. P. G. Vallabhan, *J. Phys. D* **26**, 35 (1993).
- ³⁴G. Koren and J. T. C. Yeh, *J. Appl. Phys.* **56**, 2120 (1984).
- ³⁵R. H. Dixon, R. C. Elton, and J. F. Seely, *Opt. Commun.* **45**, 397 (1983).
- ³⁶R. H. Dixon and R. C. Elton, *Phys. Rev. Lett.* **38**, 1072 (1977).
- ³⁷Y. Iida and E. S. Yeung, *Appl. Spectrosc.* **48**, 945 (1994).
- ³⁸D. L. Pappas, K. L. Saenger, J. J. Cuomo, and R. W. Dreytus, *J. Appl. Phys.* **72**, 3966 (1992).